JOURNAL OF MATERIALS SCIENCE 37 (2002) 81–88

Thermal decomposition of the ammonium zinc acetate citrate precursor for aqueous chemical solution deposition of ZnO

K. VAN WERDE, D. MONDELAERS, G. VANHOYLAND, D. NELIS, M. K. VAN BAEL, J. MULLENS, L. C. VAN POUCKE
Limburgs Universitair Centrum, Laboratory of Inorganic and Physical Chemistry, IMO, B-3590 Diepenbeek, Belgium
E-mail: jules.mullens@luc.ac.be

B. VAN DER VEKEN, H. O. DESSEYN
RUCA University Antwerp, Department of Chemistry, B-2020 Antwerpen, Belgium

The thermal decomposition of an aqueous chemical solution deposition Zn^{2+}-precursor is studied by HT-DRIFT (high temperature diffuse reflectance infrared Fourier transform spectroscopy), on-line coupled TGA-EGA (thermogravimetric analysis - evolved gas analysis by Fourier transform infrared spectroscopy (FTIR) and mass spectrometry (MS)), and HT-XRD (high temperature X-ray diffraction). Using these complementary techniques, it is found that the α-hydroxyl group of the citrate ligand plays a significant role in the decomposition pathway of the ammonium zinc acetate citrate precursor. TEM (transmission electron microscopy) shows that crystalline ZnO (zincite) is formed at 390°C, after dehydroxylation of the α-hydroxyl group and subsequent decarboxylation of the Zn^{2+}-precursor complex. Before total calcination, ZnO particles are already formed and a residual organic backbone thereby remains. The results obtained by these complementary techniques clearly indicate the importance of thermal analysis in the preparation of ceramics through chemical solution deposition.

1. Introduction

An ammonium zinc acetate citrate precursor gel was synthesized in a study to obtain a homogeneous precursor for ferroelectric $Pb(Zn_{1/3}Nb_{2/3})O_3$ by an aqueous amorphous metal carboxylate gelation method, a so called 'wet' or 'chemical precursor synthesis'. For such multicomponent metal oxide ceramics it is important to achieve a homogeneous distribution of constituent metal ions in the precursor gel [1]. It is our believe that initial cation mixing at a molecular level, leads to lower processing temperatures, shorter sintering times and more homogeneous end products: this is due to shorter diffusion distance for the constituent metal ions and molecular stoichiometry [2, 3].

However, phase segregation of one of the metal ions can occur during thermolysis of the precursor gel. This feature is caused by differences in decomposition temperature of the various carboxylatometal complexes [4]. More specific, in the case of $Pb(Zn_{1/3}Nb_{2/3})O_3$ phase segregation of ZnO is crucial, since the Zn^{2+} needs to be incorporated in the perovskite lattice in order to avoid formation of the non-ferroelectric cubic pyrochlore, lead niobate $Pb_3Nb_4O_{13}$ [5, 6]. It is for this reason that especially the thermal decomposition of the monometallic ammonium zinc acetate citrate precursor gel is investigated. This study is done by the complementary thermal analysis techniques HT-DRIFT, TGA-EGA and HT-XRD; for it has been shown previously that profound thermal analysis of monometallic precursors leads to better insight in the decompostion mechanism of multicomponent metal oxide precursors and their consequetive crystallographic phase formation [7–9].

2. Experimental

2.1. Experimental equipment and methods

HT-DRIFT measurements were performed on a Bruker IFS 66 spectrometer equipped with a high temperature-high pressure chamber with parabolic ZnSe windows (0030-011 Spectratech Inc.). A DTGS detector was used for which a resolution of 4 cm^{-1} was selected. Investigated samples were mixed with KBr in 2 w/w%. The samples were continuously flushed with a gas under consideration. Heating was controlled with a Eurotherm digital temperature controller (model 808). A heating rate of 10°C min^{-1} was chosen for every HT-DRIFT experiment.

TGA-FTIR measurements were performed with a TGA 951-2000 apparatus from TA Instruments on-line coupled to a Bruker IFS 48 FTIR spectrometer. The coupling is described elsewhere [10]. In order to identify the evolved gasses, TGA-FTIR windows were created by integrating the absorption area around

characteristic absorption bands and plotting them as a function of time [11]. In all coupled experiments a resolution of 8 cm^{-1} was selected for the MCT detector. The carrier gasses used were argon, nitrogen or an air-like mixture of O_2 and N_2 (Air Liquide) at a flow rate of 75 mL min^{-1}. Before measurements in argon or nitrogen, the inert working conditions of the TGA equipment were checked using copper oxalate as a standard [12]. TGA-MS experiments were performed by coupling the thermobalance to a quadrupole mass spectrometer (Model Thermolab of VG Fisons Instruments), using a flexible heated silica lined steel capillary and a molecular leak. In all TGA-EGA experiments a heating rate of 10°C min^{-1} was applied.

For HT-XRD measurements a modified Siemens D-5000 powder diffractometer with Cu K_α as the radiation source was used. The configuration consisted of a Göbel mirror ($K_{\alpha 1+2}$, Huber), a high temperature device with a Pt rod (Anton Paar, HTK 10) and a position sensitive detector (Braun). The Pt rod also contributes to the diffraction pattern (peaks at 39.76, 46.24 and 67.45° 2θ). For this study the equipment was operated in the hot-stage mode. It is then possible to take diffractograms *in situ* during heating of the sample in static air. Differential thermal analysis was carried out in dry air on a DTA 1600-2000 from TA Instruments. For HT-XRD and DTA a heating rate of 10°C min^{-1} was considered. TEM studies were performed on a Philips CM12 operating at 120 kV.

2.2. Materials and reagents

The following materials and reagents were used: zinc oxide (Merck, p.a. ZnO), zinc acetate dihydrate (Aldrich, 98+% $Zn(OOCCH3)_2 \cdot 2H_2O$), citric acid (Aldrich, 99% C(OH)(COOH) $(CH_2COOH)_2$), ammonia solution (UCB, p.a. NH_3 ca 25% in H_2O), transaconitic acid (Acros, 98% C(COOH) (=CHCOOH) (CH_2COOH)), itaconic anhydride (Acros, 98% $C_5H_4O_3$), itaconic acid (Aldrich, 99+% C(COOH) $(=CH_2)(CH_2COOH)$), citraconic anhydride (Acros, 98% $C_5H_4O_3$), citraconic acid (Acros, 99+% $C(COOH)(CH_3)(=CHCOOH)$).

2.3. Preparation of the precursor gels

Two different Zn^{2+}-precursor gels were prepared, as illustrated in Fig. 1. For precursor 1 ZnO was dissolved in a 0.2 mol L^{-1} citric acid solution at 65°C, the Zn^{2+}: citric acid ratio was 1:1.05. Then, the acidity was decreased by addition of ammonia until pH 8.5. At that pH the carboxylate groups of citric acid are deprotonated ($pK_{a3} = 6.39$) [13], resulting in strong interaction between citrate ($C_6H_6O_7^{\ 3-}$) and Zn^{2+}. The forthcoming 0.1 M Zn^{2+} precursor solution was poured in to a Petri vessel and the solvent was evaporated in an oven under dry air at 80°C. The resulting gel was colorless, transparent, homogeneous and amorphous, as could be seen in XRD. By means of a Kjehldahl titration [14] the total ammonia ($NH_3 + NH_4^+$) content of the dried gel was determined. For precursor 2 a similar synthesis route was followed, except for the first synthesis step, where zinc acetate dihydrate was used instead of zinc oxide. Finally, an ammonium citrate precursor (without zinc) was prepared in the same way as the ammonium zinc citrate precursor, that is, by preparing an ammonium citrate solution of pH 8.5 and evaporating the solvent at 80°C under dry air in an oven. In the same way an ammonium aconitate gel was prepared.

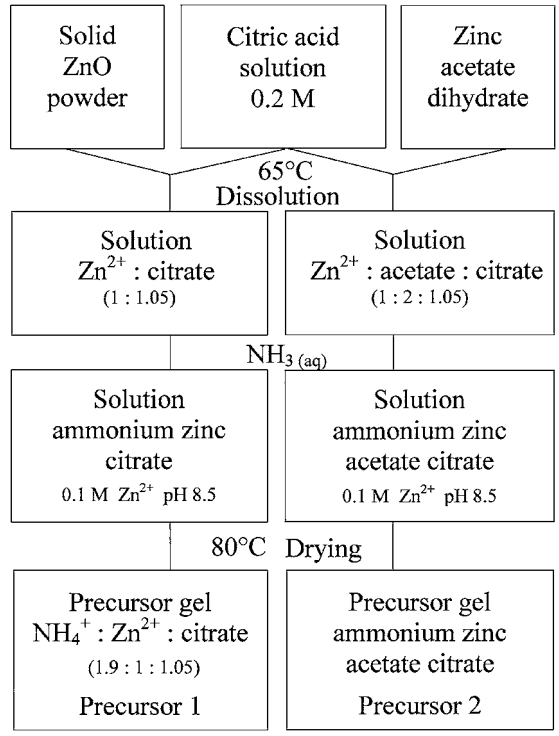

Figure 1 Synthesis route of the ammonium zinc citrate gel, left (precursor 1). Synthesis route of the ammonium zinc acetate citrate gel, right (precursor 2).

3. Results and discussion

3.1. Oxidative decomposition of citric acid and ammonium citrate in dry air

In order to understand the thermal decomposition of both Zn^{2+}-precursors, the oxidative decomposition of citric acid and the oxidative decomposition of ammonium citrate were studied in dry air.

3.1.1. Oxidative decomposition of citric acid in dry air

Although other authors investigated the decomposition pathway of citric acid by means of TGA, DTA, and TPDS (temperature programmed decomposition spectra) [15], here additional thermal analyses by TGA-FTIR and especially HT-DRIFT on citric acid and ammonium citrate were performed.

Rajendran *et al.* [15] concluded citric acid decomposes at low ramping rate (<250°C min^{-1}) via a series of endothermic dehydroxylation and decarboxylation steps with formation of respectively aconitic acid, itaconic acid, itaconic anhydride and citraconic anhydride (methyl maleic anhydride): see Fig. 2. In order to compare (confirm) this mechanism with our results, DRIFT-spectra of these citric acid derivatives were recorded at room temperature and additional HT-DRIFT and TG-FTIR measurements on citric acid in dry air were performed. The reference spectra as well as HT-DRIFT spectra are shown in Fig. 3: at room temperature the most relevant vibrations of citric acid are

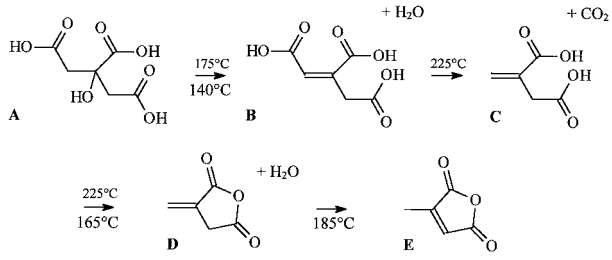

Figure 2 Thermal decomposition sequence of citric acid. Temperatures above the arrow are proposed by Rajendran *et al*. [15] for a heating rate of 25°C/min. Temperatures below the arrow are those proposed in this work.

the carbon-oxygen stretch of the α-hydroxide ($\nu_{(C-O)}$ double peak at 1075 cm^{-1}), the carbonyl stretch of the carboxylic group ($\nu_{(C=O)}$ at 1750-1700 cm^{-1}) and the hydrogen-oxygen stretch of both the α-hydroxide and the carboxylic group ($\nu_{(O-H)}$ respectively the sharp peak at 3490 cm^{-1} and the broad band around 3300–3100 cm^{-1}).

At 140°C (Fig. 3) the $\nu_{(C-O)}$ absorption of the α-hydroxide group and the sharp $\nu_{(O-H)}$ absorption disappear as a cause of dehydroxylation, resulting in an unsaturated citric acid derivative, aconitic acid. At 160°C the HT-DRIFT spectrum shows the characteristic fingerprint region of itaconic anhydride: the carbonyl stretches $\nu_{(C=O)}$ occur typically at 1850 cm^{-1} and 1780 cm^{-1}. Other characteristic itaconic anhydride absorptions are observed at 1005 cm^{-1} and 895 cm^{-1} (as compared to the reference spectra). One can even observe the carbon-hydrogen stretch $\nu_{(=C-H)}$ around 3100 cm^{-1}. This anhydride is formed through endothermic decarboxylation and anhydride formation out of aconitic acid as is stated by Rajendran *et al*. [15].

At higher temperatures another cyclic anhydride is formed. Citraconic anhydride is clearly present at 180°C as observed by typical absorptions at 980 cm^{-1} and 700 cm^{-1}. Presumably, citraconic anhydride is formed out of itaconic anhydride because of its more stable double bond. From TGA-FTIR-data we concluded these anhydrides evaporate and decompose at temperatures above 210°C in dry air (data not shown).

HT-DRIFT and TGA-FTIR on aconitic acid and itaconic acid show the same decomposition mechanism as citric acid (figures not shown). In both cases itaconic anhydride as well as citraconic anhydride are formed through endothermic decarboxylation and anhydride formation.

Additional HT-DRIFT and TGA-FTIR showed our decomposition results are in accordance with the decomposition of citric acid as proposed by Rajendran *et al*. The decomposition pathway as stated in Fig. 2 is to be considered when unraveling the decomposition mechanism of the following Zn^{2+}-precursors.

3.1.2. Oxidative decomposition of ammonium citrate in dry air

Fig. 4 shows the HT-DRIFT spectra during decomposition of ammonium citrate in dry air. At room temperature the most relevant vibrations are again the carbon-oxygen stretch of the α-hydroxide group, $\nu_{(C-O)}$ (the double peak around 1075 cm^{-1}) and the carbonyl stretch of the carboxylate group: here $\nu_{as(C=O)}$

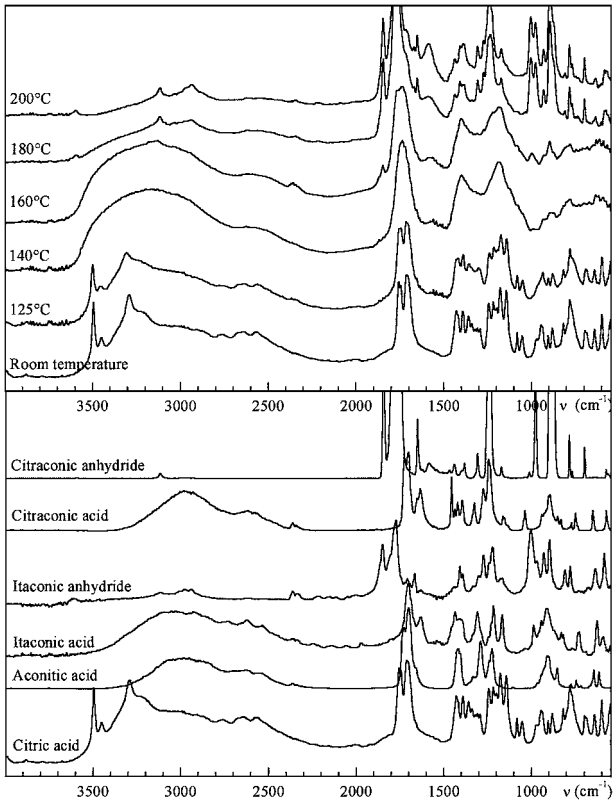

Figure 3 Upper: HT-DRIFT spectrum of decomposing citric acid in dry air at a heating rate of 10°C/min. Below: DRIFT spectra of reference compounds at room temperature (citric acid, aconitic acid, itaconic acid, itaconic anhydride, citraconic acid, citraconic anhydride).

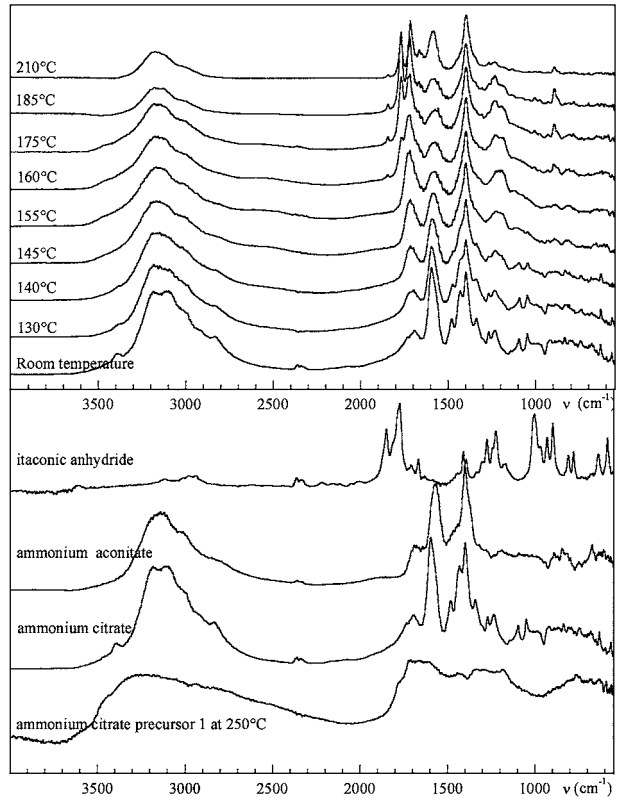

Figure 4 Upper: HT-DRIFT spectrum of decomposing ammonium citrate in dry air at a heating rate of 10°C/min. Below: DRIFT spectra of reference compounds at room temperature (itaconic anhydride, ammonium aconitate, ammonium citrate). Included is the DRIFT spectrum of ammonium citrate heated to 250°C.

and $\nu_{s(C=O)}$ occur at lower wavenumbers because of the ionic interaction between the carboxylate group and the NH_4^+-ion (respectively at 1600 cm^{-1} and at 1410 cm^{-1}) [16].

Once again the decomposition mechanism was unraveled by comparison of the HT-DRIFT spectra with the DRIFT spectra of reference compounds at room temperature (shown in Fig. 4). At 140°C ammonium citrate loses water due to the dehydroxylation of the α-hydroxide (disappearance of the $\nu_{(C-O)}$ and $\nu_{(O-H)}$). In this way ammonium aconitate is formed. At 155°C the absorption intensity of $\nu_{as(C=O)}$ and $\nu_{s(C=O)}$ starts to decrease, while the $\nu_{(C=O)}$ absorption due to free acid groups increases (1725 cm^{-1}). This happens simultaneous with the evolution of NH_3 in TGA-FTIR as shown in Fig. 5. This means the ammonium carboxylate groups in ammonium aconitate are decomposing in aconitic acid and free NH_3. Subsequently to the formation of free carboxylic acid groups and NH_3-evolution a decarboxylation of the thus formed aconitate occurs near 210°C. In TGA-FTIR one can clearly observe CO_2- evolution after NH_3 evolution. At the same time the HT-DRIFT spectra (Fig. 4) show the characteristic absorptions of the above mentioned itaconic anhydride (typical absorption at 1850 cm^{-1} and 1780 cm^{-1}). In non-oxidative atmosphere ammonium citrate shows the same feature, which indicates that the evolution of CO_2 is due to a decarboxylation process. In this way one can propose the formation of itaconic anhydride out of ammonium citrate through respectively dehydroxylation, decomposition of the ammonium carboxylates into free acid groups and NH_3, and subsequent decarboxylation.

In order to investigate the decomposition at elevated temperatures (above 250°C) a large quantity of ammonium citrate was heated in dry air in a conventional furnace up to 250°C at 10°C/min and then cooled down to room temperature. The DRIFT spectrum (Fig. 4) shows a broad absorption band (3500–2600 cm^{-1}) in the $\nu_{(N-H)}$ region with a maximum around 3200 cm^{-1}. In TGA-MS (Fig. 5) this ammonium citrate derivative shows the evolution of NO and NO_2 between 450 and 600°C, clearly indicating the presence of nitrogen-containing compounds at 250°C.

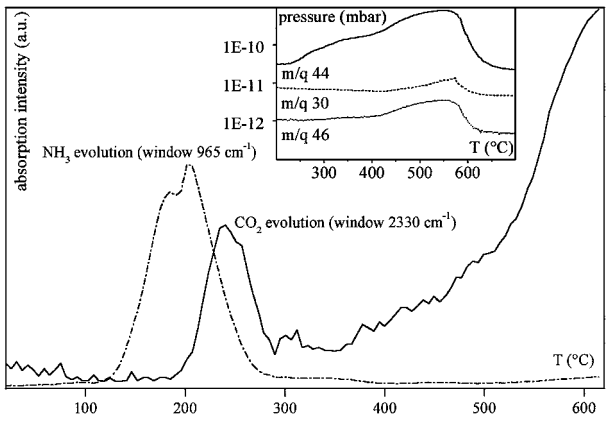

Figure 5 The evolution of NH_3 (dash dotted line; window at 965 cm^{-1}) and CO_2 (full line; window at 2330 cm^{-1}) is shown for ammonium citrate by TGA-FTIR in dry air at a heating rate of 10°C/min. The integrated picture shows the TGA-MS evolution of m/q 46 (NO_2), m/q 30 (NO) and m/q 44 (CO_2) of the preheated ammonium citrate sample at 10°C/min in dry air.

It is our believe that during the above mentioned NH_3-evolution (155–250°C) (poly-) amides and/or (cyclic) imides are formed (cyclic imides show typical intense $\nu_{(N-H)}$ absorption at 3225–3125 cm^{-1} as well as broad carbonyl absorption $\nu_{(C=O)}$ at 1695 cm^{-1} [17]). Nevertheless all the remaining products at 250°C, including the anhydrides and the amides or imides, decompose at temperatures between 300 and 650°C (as shown in TGA-MS, Fig. 5).

3.2. Oxidative decomposition of the Zn^{2+}-precursors

3.2.1. Oxidative decomposition of the ammonium Zn^{2+}-citrate precursor (precursor 1) in dry air

In order to understand the decomposition mechanism of the ammonium Zn^{2+}- acetate citrate precursor (precursor 2) we first had to investigate the interaction between the strongest ligand bond, the citrate ion, and Zn^{2+}. It is known that the α-hydroxide group of citric acid plays an important role in the gelation and subsequent decomposition pathway of the metal-citrate precursor or other metal-α-hydroxy-carboxylate precursors [18]. Therefore an ammonium Zn^{2+}-citrate precursor (precursor 1; without any acetate ions) was investigated at first. In section 3.4. acetate ions are introduced into the system and their role will be discussed. The decomposition pathway is divided into three major areas, as distinguished in DTA and TGA (Fig. 6). The first part of the decomposition path (below 280°C) only contains endothermic processes in dry air, while the second part (between 280°C and 420°C) contains an exothermic reaction in dry air. The final part (above 420°C) shows highly exothermic processes in dry air. In the next section, each of the decomposition areas will be discussed in more detail.

The HT-DRIFT spectra of precursor 1 are shown in Fig. 7. At room temperature only coordinated carboxylates, either by NH_4^+ or Zn^{2+} are present ($\nu_{as(C=O)}$ at 1600 cm^{-1}, $\nu_{s(C=O)}$ at 1420 cm^{-1}). A separation energy of $\Delta = 180$ cm^{-1} between $\nu_{as(C=O)}$ and $\nu_{s(C=O)}$ indicates that the carboxylate group of the citrate ion forms either an ionic bond to one Zn^{2+}-ion or acts as a bridge between two Zn^{2+}-ions [19]. A second feature of the precursor at room temperature is the characteristic carbon-oxygen stretch $\nu_{(C-O)}$ of the α-hydroxide group: the appearance of a broad band around 1090 cm^{-1} instead of a doublet (which was the case for citric acid and ammonium citrate) might indicate the α-hydroxid group is chemically bound in a different way or is otherwise under a lot of strain.

In the first decomposition area, beneath 110°C the precursor loses adsorbed water. This is indicated by a small endothermic peak in DTA and the evolution of H_2O at m/q 18 in TGA-MS, as shown in Fig. 6. At a slightly higher temperature, at about 140°C, NH_3 starts to evolve from the precursor gel. All TGA-MS experiments were performed with an ionization energy of 20 eV. In that way we were certain to distinguish NH_3^+ from OH^+ at m/q 17, since low ionization energy inhibits the creation of OH^+-ions (m/q 17) [20]. In TGA-MS (Fig. 6) the NH_3-evolution reaches a first maximum

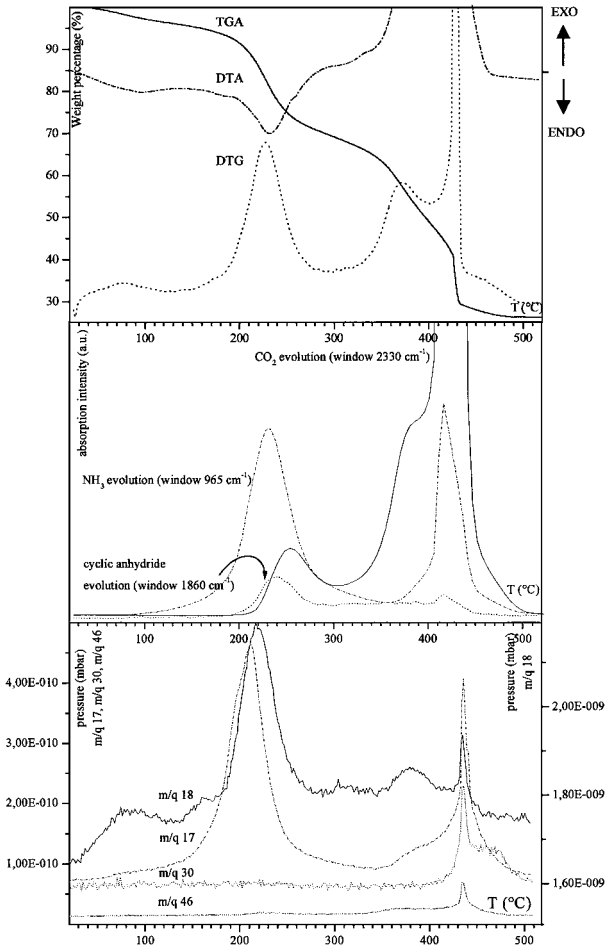

Figure 6 TGA-EGA of the ammonium zinc citrate gel in dry air. Upper: TGA in dry air at 10°C/min (full line) and corresponding DTG (dotted line), DTA in dry air at 10°C/min (dash dotted line). Center: TGA-FTIR windows showing the evolution of NH_3 (dash dotted line; window at 965 cm^{-1}, CO_2 (full line; window at 2330 cm^{-1}) and cyclic anhydrides (dotted line; window at 1860 cm^{-1}) in dry air at 10°C/min. Below: TGA-MS showing the evolution of m/q 18 (H_2O), m/q 17 (NH_3), m/q 30 (NO) and m/q 46 (NO_2). An ionization energy of 20 eV was used in TGA-MS.

near 230°C (which can also be seen in TGA-FTIR). At that temperature, the HT-DRIFT spectrum (Fig. 7) clearly features some free acid groups at 1720 cm^{-1}. The appearance of these free carboxylic acids, the evolution of NH_3 and a clear endothermic process in DTA indicate the endothermic decomposition of ammonium carboxylate groups as was previously shown

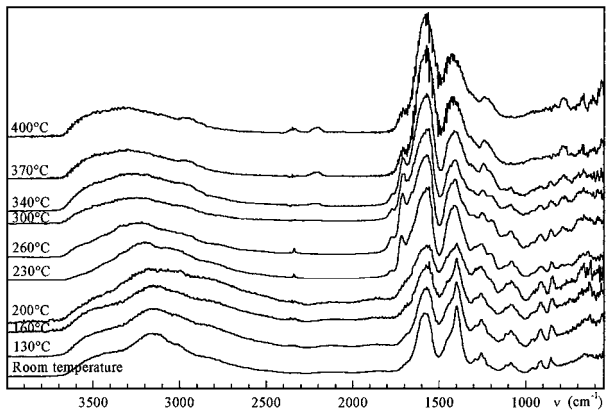

Figure 7 HT-DRIFT spectra of decomposing ammonium zinc citrate in dry air at a heating rate of 10°C/min.

for ammonium citrate. However, compared to ammonium citrate only very few cyclic anhydrides are formed by a subsequent decarboxylation: in HT-DRIFT (Fig. 7) very little itaconic anhydride is observed ($\nu_{(C=O)}$ at 1860 cm^{-1} and 1780 cm^{-1}). In TGA-FTIR a very small evolution around 250°C indicates some evolving cyclic anhydrides, probably coming from the 5% excess citric acid used in the precursor synthesis. Moreover, as opposed to ammonium citrate, the $\nu_{(C-O)}$ absorption of the α-hydroxide group remains present far beyond 140°C, undoubtedly indicating a different bond of the α-hydroxide. Both these phenomena: the absence of cyclic anhydrides and the remaining presence of the α-hydroxide group, state a chemical bond between Zn^{2+} and the α-hydroxide group. This interaction prohibits the formation of an aconitate and the subsequent formation of its derived anhydrides.

In the second decomposition region the α-hydroxide group remains visible in the HT-DRIFT spectrum (Fig. 7) until 340°C. At that moment one can observe H_2O-evolution in TGA-MS (Fig. 6). At the same time TGA-FTIR shows a second CO_2 evolution starting at 340°C. It is presumed that these processes are respectively a dehydroxylation and subsequent decarboxylation of the Zn^{2+}-precursor complex. Both reactions also occur in inert atmosphere: Fig. 8 shows the TGA, DTG and TGA-FTIR of the ammonium Zn^{2+} citrate precursor in argon at a heating rate of 10°C/min. The occurrence of CO_2-evolution, starting at 340°C, in argon, indicates the CO_2-evolution in dry air is a decarboxylation process and not an oxidative decomposition. The

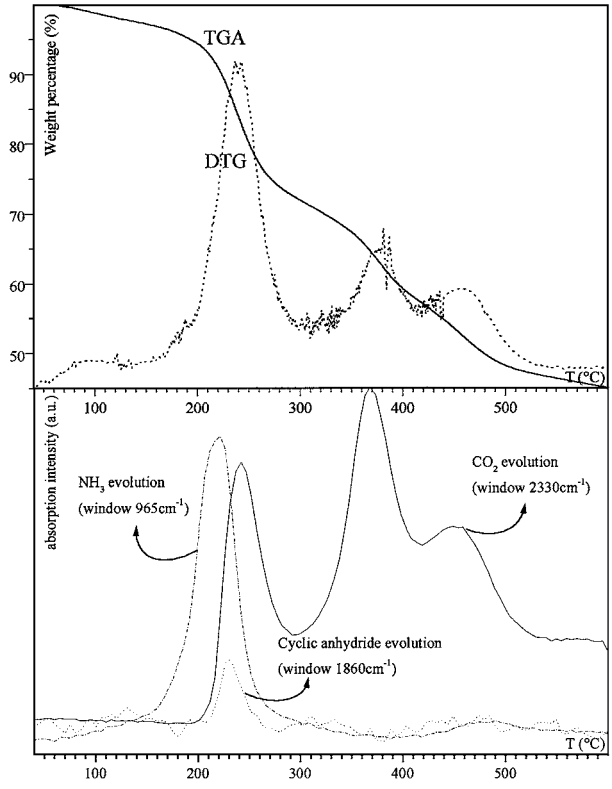

Figure 8 TGA-FTIR of the ammonium zinc citrate gel in argon. Upper: TGA at 10°C/min in argon (full line) and corresponding DTG (dotted line). Below: TGA-FTIR windows showing the evolution of NH_3 (dash dotted line; window at 965 cm^{-1}), CO_2 (full line; window at 2330 cm^{-1}) and cyclic anhydride (dotted line; window at 1860 cm^{-1}) in argon at 10°C/min.

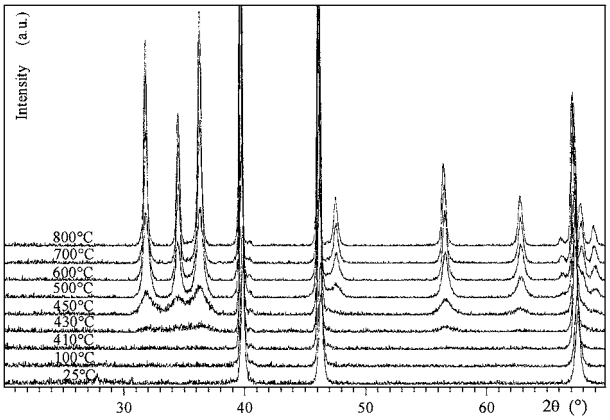

Figure 9 HT-XRD spectra of the ammonium zinc citrate gel. The intense Bragg-reflections at 39.8°, 46.2° and 67.5° 2θ are due to the platinum sample holder.

copper oxalate test was used to assure the inertness of the atmosphere for the experiments in argon [12].

As a consequence of the above dehydroxylation and the subsequent decarboxylation of the Zn^{2+}-precursor complex, the Zn^{2+}-ion gets decoordinated by its ligand and ZnO is formed. Fig. 9 shows the HT-XRD spectra of precursor 1 in dry static air. Here it is shown that this precursor is amorphous during decomposition up to 410°C (the intense Bragg-reflections at 39.8°, 46.2° and 67.5° 2θ are due to the platinum sample holder). The diffraction pattern at 430°C clearly shows the initial formation of ZnO, as designated by JCPDS-database. It is important to note crystallographic particles only diffract constructively starting from a certain size. This means crystalline ZnO (zincite) was already formed at lower temperature ($T < 430$°C). To verify this statement a thin film of the Zn^{2+} precursor solution was deposited on a copper TEM-grid. This grid was then heated up in a TGA-furnace until 390°C in dry air at 10°C/min. In TEM small particles of about 10 to 20 nm in size were observed in the free standing film (Fig. 10). The electron diffraction pattern confirmed that they consisted of ZnO. Therefore one can conclude the dehydroxylation and subsequent decarboxylation process of the precursor complex result in the formation of ZnO particles. Zincite is thereby formed before the calcination temperature, which means that the oxide is formed before all organic material has decomposed: an organic rest remains surrounding these oxide particles.

The final part of the decomposition pathway contains the oxidative burning out of the organic residue. DTA, TGA-MS and TGA-FTIR (Fig. 6.) show the exothermic decomposition of the remaining organic backbone at 430°C in dry air. A large quantity of CO_2 evolves. TGA-MS at m/q 30 and 46 show the evolution of nitrogen oxides, indicating the presence of nitrogen containing organics, as is the case for the ammonium citrate decomposition. As seen in Fig. 6 even more ammonia is released. The HT-DRIFT spectra (Fig. 7) of the precursor above 230°C show energetic nitrogen-hydrogen stretching vibrations $\nu_{(N-H)}$ around 3300 cm^{-1}. All of these techniques indicate the presence of imides and especially amides in the organic backbone, probably formed by reaction of ammonia and free carboxylic acid groups around 230°C (during evolution of NH_3).

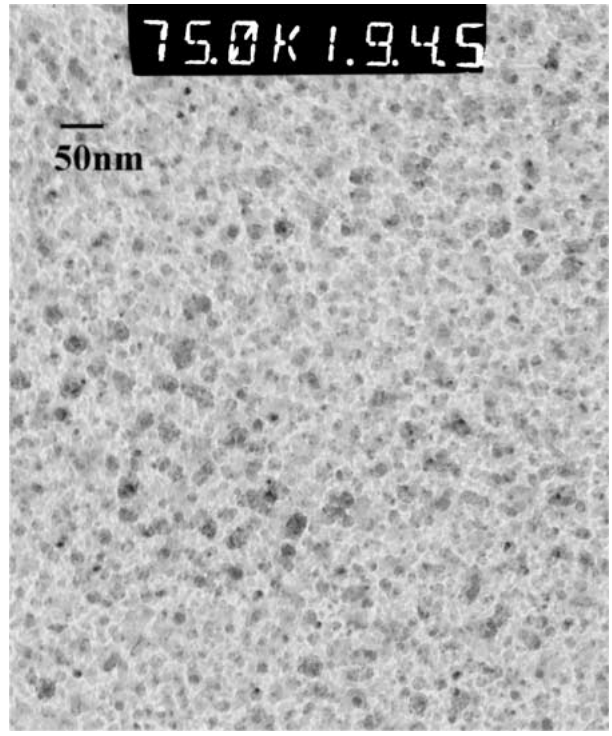

Figure 10 Transmission electron microscopic picture of an ammonium zinc citrate gel film heated up to 390°C, supported by a copper TEM-grid.

After complete decomposition in dry air the remaining weight percentage at 500°C is 26.5%, in good accordance with the theoretical value of 27.1% for ZnO. In non-oxidative argon flow, the resulting weight percentage is 49% due to the incomplete oxidation of the organic backbone. Although the above mentioned copper oxalate test showed there is no oxidation caused by atmospheric oxygen, there still is some CO_2-evolution during the TGA-FTIR (and TGA-MS) experiment in argon at 430°C. The reason for this is that the oxygen present in the oxygen rich backbone is used for the burning of some remaining organics.

3.2.2. Oxidative decomposition of the ammonium Zn^{2+} acetate citrate precursor (precursor 2) in dry air

The decomposition pathway of this precursor gel is very similar to that of precursor 1. Fig. 11 shows respectively the TGA, DTG and TGA-FTIR of the ammonium Zn^{2+}-acetate citrate precursor. Precursor 2 shows the same three decomposition area's, featuring the same processes. From TGA-FTIR it is concluded that two kinds of acetate ions are involved. One has to distinguish between acetate ions bound to Zn^{2+} and those bound to ammonium. The last mentioned, the ammonium acetate molecules in the gel, decompose in the form of acetic acid and NH_3 at 170°C. At that temperature both gases are released simultaneously, as detected in TGA-FTIR (Fig. 11). The fraction acetate ions bound to Zn^{2+} do not evolve until 290°C. At that temperature there is no evolution of ammonia.

Nevertheless there are some small differences between precursor 1 and 2. For precursor 2 more NH_3 evolves in the final step and the temperature at which this step occurs lies higher (480°C). Although these

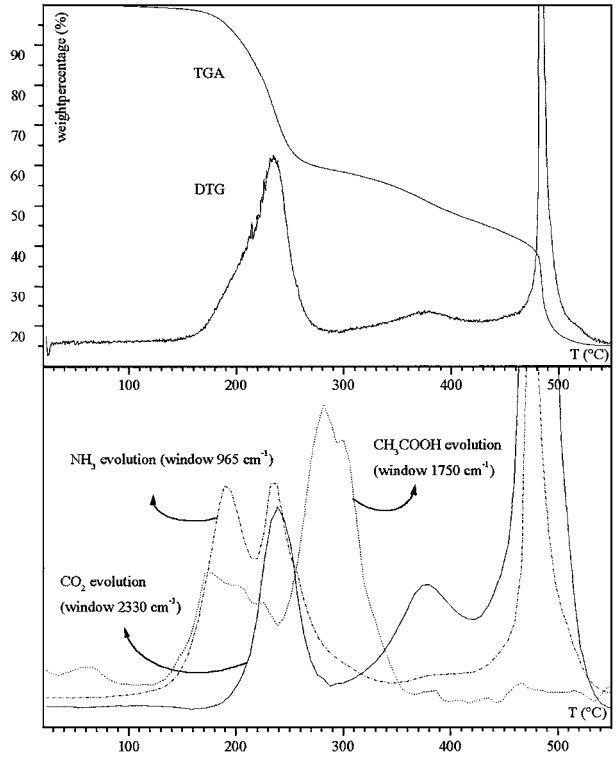

Figure 11 TGA-FTIR of the ammonium zinc acetate citrate gel in dry air. Upper: TGA at 10°C/min in argon and corresponding DTG. Below: TGA-FTIR windows showing the evolution of NH_3 (dash dotted line; window at 965 cm^{-1}), CO_2 (full line; window at 2330 cm^{-1}) and acetic acid (dotted line; window at 1750 cm^{-1}) in dry air at 10°C/min.

features need further investigation, it seems reasonable to assume that there is less intermolecular Zn^{2+}-citrate interaction between two nearby complexes in precursor 2. The carboxylate bond between one Zn^{2+} ion and another nearby zinc citrate ion is probably substituted by a bond between that Zn^{2+} and an acetate ion. Because of that, more free ammonium carboxylate groups are formed in the gel and more amide/imide groups can be formed during thermal decomposition, resulting in a stronger backbone and more intense NH_3 evolution.

4. Conclusions

For both new chemical solution deposition Zn^{2+}-precursors the thermal decomposition mechanism was unraveled. Thermal analysis showed the characteristics and the importance of the α-hydroxyl group of the citrate ligand. That is: both the Zn^{2+}-precursors are stable until the α-hydroxyl group dehydrolyses from the complex. Crystalline ZnO is formed directly after dehydroxylation and decarboxylation of the complex, and this before the precursor is completely calcinated. This crystallization is extremely important, since crystalline zincite already forms at lower temperature than the decomposition step of the organic backbone.

If these Zn^{2+}-precursors are to be used in the aqueous synthesis of multi metalion ceramics, such as $Pb(Zn_{1/3}Nb_{2/3})O_3$, the thermal decomposition of all metal complexes should be profoundly investigated, since metal oxides can already be formed before total calcination. It is not sufficient to conclude the metal oxide is formed at the final precursor decomposition step only by interpreting a TGA measurement. This could lead to phase segregation when incorporating this precursor in a multicomponent metal oxide precursor synthesis.

Thermal analysis also shows the influence of the acetate ion on the precursor decomposition: it increases the final decomposition step to a slightly higher temperature and causes a more substantial evolution of ammonia in the final step. This is presumably caused by the greater extent to which amides and imides are formed in the organic backbone during thermal decomposition.

Acknowledgments

K. Van Werde is indebted to the 'Vlaams instituut voor de bevordering van het wetenschappelijk technologisch onderzoek in de industrie' (IWT). G. Vanhoyland and D. Nelis are research assistants of the Fund for Scientific Research Flanders, Belgium (FWO). M. K. Van Bael is a post doctoral fellow of the Fund for Scientific Research Flanders, Belgium (FWO).

References

1. R. NOUWEN, J. MULLENS, D. FRANCO, J. YPERMAN and L. C. VAN POUCKE, *Vibrational Spectroscopy* **10** (1996) 291.
2. M. K. VAN BAEL, E. KNAEPEN, A. KAREIVA, I. SCHILDERMANS, R. NOUWEN, J. D'HAEN, M. D'OLIESLAEGER, C. QUAEYHAEGENS, D. FRANCO, J. YPERMAN, J. MULLENS and L. C. VANPOUCKE, *Supercond. Sci. Technol.* **11** (1998) 82.
3. M. K. VAN BAEL, A. KAREIVA, R. NOUWEN, I. SCHILDERMANS, G. VANHOYLAND, J. D'HAEN, M. D'OLIESLAEGER, D. FRANCO, J. YPERMAN, J. MULLENS and L. C. VAN POUCKE, *Int. J. Inorg. Mater.* **1** (1999) 259.
4. Y. NARENDAR and G. L. MESSING, *Catalysis Today* **35** (1997) 247.
5. N. WAKIYA, K. SHINOZAKI and N. MIZUTANI, *J. Amer. Ceram. Soc.* **80**(12) (1997) 3217.
6. T. R. SHROUT and A. HALLIYAL, *Am. Ceram. Soc. Bull.* **66**(4) (1987) 704.
7. G. VANHOYLAND, R. NOUWEN, M. K. VAN BAEL, J. YPERMAN, J. MULLENS and L. C. VAN POUCKE, *Thermochimica Acta* **354** (2000) 145.
8. E. KNAEPEN, M. K. VAN BAEL, I. SCHILDERMANS, R. NOUWEN, J. D'HAEN, M. D'OLIESLAEGER, C. QUAEYHAGENS, D. FRANCO, J. YPERMAN, J. MULLENS and L. C. VAN POUCKE, *ibid.* **318** (1998) 143.
9. S. A. A. MANSOUR, *ibid.* **233** (1994) 257.
10. J. MULLENS, R. CARLEER, G. REGGERS, J. YPERMAN, J. VANHEES and L. C. VAN POUCKE, *ibid.* **212** (1992) 219.
11. J. MULLENS, in "Handbook of Thermal Analysis and Calorimetry," Vol.1., edited by M. Brown and P. Gallagher (Elsevier, Amsterdam, 1998) p. 509.
12. J. MULLENS, A. VOS, R. CARLEER, G. REGGERS, J. YPERMAN and L. C. VAN POUCKE, *Thermochimica Acta* **207** (1992) 337.
13. R. C. WEAST (ed.), "CRC Handbook of Chemistry and Physics," 52nd ed. (Chemical Rubber Company, Cleveland, Ohio, 1971/1972).
14. A. I. VOGEL, in "Textbook of Quantitative Chemical Analysis," 5th ed., revised by G. H. Jeffrey, J. Besset, J Mendham and R. C. Denney (Longman Scientific & Technical, London, 1989) p. 302.
15. M. RAJENDRAN and M. S. RAO, *J. Solid State Chem.* **113** (1994) 239.
16. C. J. POUCHERT, in "The Aldrich Library of Infrared Spectra," 2nd ed. (Aldrich Chemical Company, Inc., Wisconsin, 1975).

17. N. B. COLTHUP, L. H. DALY and S. E. WIBERLY, in "Introduction to Infrared and Raman Spectroscopy," 3rd ed. (Academic Press, New York).
18. J. LIVAGE, M. HENRY and C. SANCHEZ, *Prog. Solid. St. Chem.* **18** (1988) 259.
19. K. NAKAMOTO, in "Infrared & Raman Spectroscopy of Inorganic and Coordination Compounds, Part B.: Application in Coordination, Organometallic and Bioinorganic Chemistry," 5th ed. (J. Wiley & Sons, New York, 1997).
20. "Thermolab Instruction Manual: Evolved Gas Analyser for Thermal Analysis—Mass Spectrometry" (Fisons Instruments) p. 37.

Received 23 January
and accepted 25 July 2001